Imidazolium-Based Ionic Liquids: Quantitative Aspects in the Far-Infrared Region

Thierry Buffeteau,* Joseph Grondin, Yann Danten, and Jean-Claude Lassègues

Institut des Sciences Moléculaires, UMR 5255, CNRS, Université Bordeaux I, 351 Cours de la Libération, 33405 Talence Cedex, France

Received: March 8, 2010; Revised Manuscript Received: May 4, 2010

The optical constants of some imidazolium-based ionic liquids (ILs) are determined in the mid- and far-infrared regions by combining polarized attenuated total reflection (ATR) and transmittance spectra. The internal vibrations of the cations and anions and the interionic vibrations can thus be quantitatively evaluated. A comparison of the far-IR spectral response of several imidazolium derivatives associated with the $(CF_3SO_2)_2N^-$ anion shows that methylation of the more acidic $C_{(2)}H$ imidazolium group does not change the far-IR intensity and hence that the CH···anion hydrogen bonds play a negligible role compared with electrostatic interactions. The calculated spectra of ion-pair dimers reproduce the far-IR density of states better than those of simple ion pairs.

Introduction

The optical constants, namely, the refractive index $n(\nu)$ and extinction coefficient $k(\nu)$, constitute the most fundamental quantitative information that can be obtained in the infrared (IR) domain on the vibrational properties of any isotropic liquid.[1] We have recently determined the optical constants of ionic liquids (ILs) composed of 1-butyl-3-methylimidazolium cation (BMI^+) and of the $(CF_3SO_2)_2N^-$, BF_4^-, or PF_6^- anions in the 4000−650 cm^{-1} mid-IR region.[2] The first objective of the present work is to extend this determination down to 40 cm^{-1} to connect quantitatively the far-IR results to those obtained in the literature using terahertz (THz) and dielectric spectroscopies.[3−15] The analysis of the far-IR spectra is also expected to bring its contribution to the general debate of the ILs intermolecular dynamics in a frequency and time domain where other spectroscopic approaches, such as Raman scattering,[16] inelastic neutron scattering,[17] or optical heterodyne-detected Raman-induced Kerr effect (OHD-RIKES),[18,19] provide their own specific and complementary information. A second objective is to obtain sufficiently accurate profiles to allow the response of different ILs to be compared. This is particularly difficult to achieve in the far-IR because the contribution of interionic motions that becomes predominant in this region is broad, featureless, and of weak intensity. Furthermore, a cutoff of the far-IR profile is unavoidable at low wavenumbers for instrumental reasons (40 cm^{-1} in our case). A method is proposed to overcome this difficulty and to determine the optical constants in the 4000−40 cm^{-1} region. Finally, the comparison of the different ILs is focused on the far-IR profiles, which reflect directly the local structures and interactions in these liquids.

Experimental Methods

Materials. In addition to the [BMI][BF_4], [BMI][PF_6], and [BMI][TFSI] compounds where $TFSI^-$ is the bis(trifluoromethanesulfonyl)imide anion, $(CF_3SO_2)_2N^-$, we have investigated the [MMI][TFSI], [EMI][TFSI], and [BMMI][TFSI] derivatives where MMI is the 1,3-dimethyl-imidazolium, EMI is the 1-ethyl-3-methyl-imidazolium, and BMMI is the 1-butyl-2,3 dimethyl-imidazolium. The far-IR spectrum of the *N*-butyl-*N*-trimethyl-ammonium bis(trifluoromethane-sulfonyl)imide compound [$NBuMe_3$][TFSI] has also been recorded for comparison with the imidazolium-based ILs. All of these ILs (Solvionic, 99.9%) were used as received but always stored and handled in a drybox filled with argon. Some of their properties, including the melting temperature, are reported in Table 1.

TABLE 1: Refractive Indices, *n*, in the Visible, Molarities, and Melting Temperature of the Investigated ILs

sample	refractive index 298 K	*M* (g)	*d* (g cm^{-3}) 298 K	*c* (mol dm^{-3}) 298 K	melting temp (°C)
[MMI][TFSI]	1.422	377.25	1.559[20]	4.13	26
[EMI][TFSI]	1.4231	391.31	1.5147[21]	3.87	−16
[BMI][TFSI]	1.428	419.36	1.436[21]	3.42	−4
[BMMI][TFSI]	1.4305	433.41	1.417[20]	3.27	≥20[a]
[BMI][PF_6]	1.409	284.18	1.3637[21]	4.80	8
[BMI][BF_4]	1.4215	226.06	1.1994[21]	5.31	−75
[$NBuMe_3$][TFSI]	1.4277	396.37	1.41	3.56	7

[a] Not exactly known, but this IL is liquid at room temperature.

IR Measurements. The mid- and far-IR spectra of the ILs at room temperature were recorded with a ThermoNicolet 6700 Nexus at a resolution of 4 cm^{-1}. Attenuated total reflectance (ATR) experiments were performed in the mid-IR using a single reflection ATR accessory (Specac) equipped with a germanium crystal and a liquid nitrogen cooled narrow-band mercury cadmium telluride (MCT) detector. A BaF_2 wire grid polarizer was added to record the spectra in the p and s polarizations. This experimental setup limits the spectra to 650 cm^{-1}.

Cesium iodide (CsI) and poly(ethylene) (PE) windows were used to record the spectra in the transmission mode. A film of ∼1 μm thick was spread between two CsI windows to cover the 4000−200 cm^{-1} range: two spectra were recorded in the 4000−400 and 700−200 cm^{-1} spectral ranges using the mid-IR and far-IR spectrometer configurations, respectively. A Eurolabo cell equipped with lead spacers of 25 or 50 μm and PE windows was used to cover the 600−40 cm^{-1} range. Although the investigated ILs are liquid at room temperature, they are very viscous, and great care was taken to obtain an

* To whom correspondence should be sent. E-mail: t.buffeteau@ism.u-bordeaux1.fr.

10.1021/jp102087m
Published on Web 05/14/2010

homogeneous filling of the cells without any bubble. With the BF_4 derivatives, the transmittance spectra with CsI windows have to be recorded immediately to avoid ionic exchanges. Transmission experiments performed in this study have been plotted in absorbance units ($A = -\log T$).

Spectral Simulations. The computer program used to calculate the transmittance (or absorbance) spectra of liquids is based on the Abelès matrix formalism.[22,23] This formalism takes into account the multiple reflections inside each layer (sample and cell's windows), which is characterized by a 2 × 2 matrix connecting the electric and magnetic fields at the upper and lower sides of the layer. The method has been extended to multilayer systems presenting layers with phase incoherence.[24] This extension is particularly important to compare experimental and calculated spectra for multilayer systems presenting very thick layers. Indeed, when some layers in the stratified system are sufficiently thick (cell's windows for example) so that the period of the interference is smaller than the resolution of the spectrometer, the layer interference does not appear on the experimental spectrum and should not be calculated. It is noteworthy that this 2 × 2 matrix method can be easily generalized for anisotropic layers, as shown by Yamamoto and Ishida.[25]

Determination of Optical Constants. The optical constants can be determined from only one experiment, such as ATR or transmittance at normal incidence, using the interdependence of $n(\nu)$ and $k(\nu)$ by the Kramers−Kronig relations.[26−32] The transmission method is particularly valuable for weak and moderately strong bands, whereas the ATR method can be applied to strong bands using a correction algorithm developed by Dignam et al.[28] We have shown in our previous study that ATR was the only way to determine accurately the IL optical constants in the mid-IR region because of the strong intensity of the anion absorption bands.[2] Transmittance (or absorbance) spectra need sample thicknesses of <1 μm that are difficult to control and reproduce, whereas in the ATR experiment, the thickness probed by the IR beam is directly given by the penetration depth of the evanescent wave in the sample (i.e., 0.2 to −0.3 μm for germanium crystal). The ATR method cannot be used in the far-IR region because of the nontransparency of our experimental setup. Its sensitivity would be anyway limited to detect absorptions that are ∼2 orders of magnitude weaker than in the mid-IR. Transmission experiments with sample thicknesses of about 25−50 μm are necessary, but the control and reproducibility of these thicknesses is again not easy to achieve using standard demountable cells equipped with PE windows. Therefore, we have used the optical constants determined from the ATR spectra in the 4000−650 cm^{-1} region to calculate an absorbance spectrum corresponding to a thickness of 2000 Å. Then, we have combined this absorbance spectrum calculated from ATR experiments with experimental absorbance spectra measured with CsI and PE windows. It is noteworthy that the experimental absorbance spectra, recorded with higher thicknesses, were normalized to obtain similar intensity for the absorption bands located in the overlapping regions. Finally, the optical constants were determined from this "reconstructed" absorbance spectrum using the following iterative procedure.

A first estimation of the optical constants is obtained using approximate equations of absorbance spectrum. Indeed, using the thin film approximation ($d \ll \lambda$), the normalized absorbance (i.e., absorbance spectrum subtracted from the absorbance spectrum of the substrate) is given by[30]

$$A^{\mathrm{norm}}(\nu) = A(\nu) - A^{\mathrm{sub}}(\nu) = -\log \times \left[1 - \frac{4\pi\nu d}{(1 + n_s)} \mathrm{Im}[\hat{\varepsilon}(\nu)]\right] \quad (1)$$

where n_s is the refractive index of the cell's window, d is the film thickness (2000 Å), and $\hat{\varepsilon}(\nu) = \hat{n}^2(\nu)$ is the complex dielectric constant of the film. The imaginary part of the dielectric function, $\varepsilon''(\nu) = 2n(\nu)k(\nu)$, is obtained from eq 1, and its real part, $\varepsilon'(\nu) = n^2(\nu) - k^2(\nu)$, is calculated by Kramers−Kronig transformation of the imaginary part. The initial real and imaginary parts of the dielectric function are used for calculating normalized absorbance using the Abelès formalism. Then, the imaginary part of the dielectric function is perturbed for each wavenumber by a Newton−Raphson method until the simulated and "reconstructed" spectra are sufficiently close to each other. Because the real part of the dielectric function is not perturbed, this procedure must be repeated several times until no significant changes on the real and imaginary parts of the dielectric function are observed. Finally, the final optical constants are calculated by simple arithmetical equations using the real and imaginary parts of the dielectric function

$$\mathrm{n}(\nu) = \sqrt{0.5(\sqrt{\varepsilon'^2(\nu) + \varepsilon''^2(\nu)} + \varepsilon'^2(\nu))} \quad (2)$$

$$\mathrm{k}(\nu) = \sqrt{0.5(\sqrt{\varepsilon'^2(\nu) + \varepsilon''^2(\nu)} - \varepsilon'^2(\nu))} \quad (3)$$

DFT Calculations. They have been carried out using the Gaussian 03 program[33] for the free imidazolium cations and TFSI anion for single ion-pairs IP and for ion-pair dimers $(IP)_2$. The calculated structures have been determined using the B3LYP functional with the 6-31+G(d,p) basis set. Then, the vibrational transitions have been calculated according to the harmonic force field approximation. The choice of a basis set having a fairly good quality to describe interactions in ILs precludes the vibrational analysis of clusters containing a greater number of ion pairs.

It is well known that the potential energy surface for IPs is extremely complicated and involves many local energy minimum structures with comparable interaction energy values.[34] The minimum energy structure was selected for simplicity without considering the possible contribution of other structures of similar energy to the vibrational spectra. In contrast, even if the $(IP)_2$ potential energy surface is again sophisticated, a local minimum energy structure could be unambiguously determined. Although the IP and $(IP)_2$ species remain undoubtedly oversimplified pictures of the structural organization in ILs, the localization of a minimum energy structure and the appearance of cooperative effects between ions make $(IP)_2$ species somewhat more realistic than simple IPs, as already pointed out in previous spectroscopic studies.[35]

Results

The strategy described above to determine the optical constants is illustrated in Figure 1 for the [BMI][TFSI] sample. After the optical constants have been extracted from the s-polarized ATR spectra in the 4000−650 cm^{-1} region using the previously published method[2] and the refractive indices of Table 1, the absorbance spectrum of a 2000 Å thick sample is calculated (Figure 1a). The sample thicknesses corresponding to the absorbance spectra b−d of Figure 1 are not accurately

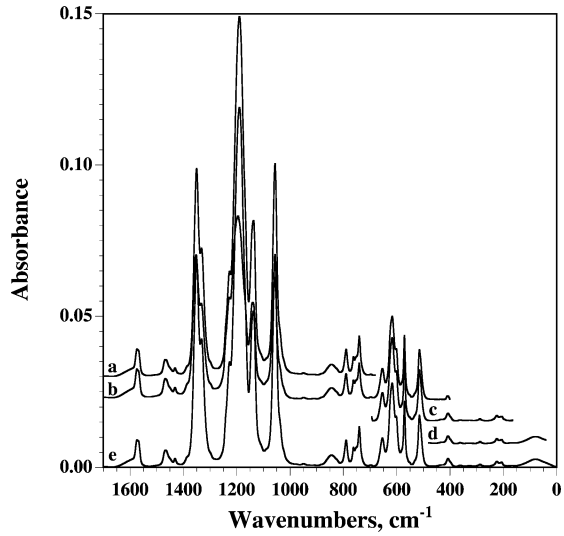

Figure 1. (a) Absorbance spectrum calculated using the [BMI][TFSI] optical constants (determined from ATR experiments) for a thickness of 2000 Å. (b) Normalized absorbance spectrum recorded with mid-IR configuration for a [BMI][TFSI] film between two CsI windows. (c) Normalized absorbance spectrum recorded with far-IR configuration for a [BMI][TFSI] film between two CsI windows. (d) Normalized absorbance spectrum of [BMI][TFSI] recorded with far-IR configuration using PE windows. (e) Reconstructed IR absorbance spectrum of a [BMI][TFSI] film 2000 Å thick. Spectra a−d have been shifted upward for convenience.

known. This is expected for a liquid film between two CsI windows (spectra b and c), but even the presence of a spacer between the PE windows does not guarantee a reproducible thickness after screwing the cell because of the limited rigidity of the PE windows (spectrum d). Therefore, experimental absorbance spectra b−d are matched to the calculated absorbance spectrum a to obtain similar intensity for the absorption bands located in the overlapping regions.

In principle, a Kramers−Kronig transformation should allow the optical constants to be evaluated from the reconstructed spectrum. However, the Kramers−Kronig transformation implies integrations over an infinite spectral range. The truncation at high wavenumbers is not a serious problem because the extinction coefficient $k(\nu)$ becomes negligibly small and the refractive index $n(\nu)$ tends toward its asymptotic value in the visible. The truncation at low wavenumbers is potentially more problematic for absorptions situated close to the cutoff. A weak and broad absorption, located at 80 ± 10 cm^{-1}, is systematically present in the far-IR for all of the ILs we have investigated. The cutoff at 40 cm^{-1} occurs on the low wavenumber side of this absorption band. To fill the 40−0 cm^{-1} region, we have considered first that the absorbance at $\nu = 0$ cm^{-1} must be zero because the absorbance is proportional to $k\nu$ and second that the THz spectra available in the literature exhibit a quasi-linear decrease in the considered zone.[9,15] Therefore, we have approximated the 40−0 cm^{-1} range by a straight line starting from the absorbance value at 40 cm^{-1} and going to zero at 0 cm^{-1}. It must be emphasized that this linear approximation is not intended to extract information from the 40−0 cm^{-1} region but just to improve the Kramers−Kronig transformation above 40 cm^{-1}. Finally, the reconstructed absorbance spectrum used to determine the optical constants of [BMI][TFSI] from the iterative procedure presented in the Experimental Methods is reported in Figure 1 (spectrum e), and the corresponding optical constants are given in Figure 2. The optical constants for the other investigated ILs are reported in the Supporting Information (Figures S1−S6).

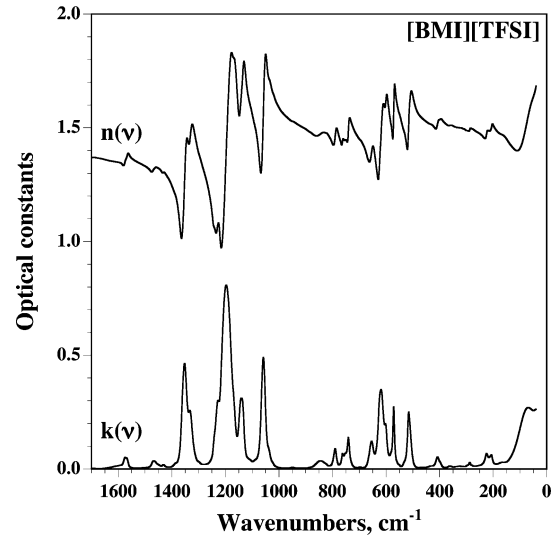

Figure 2. Optical constants of [BMI][TFSI] in the 1700−40 cm^{-1} region at room temperature.

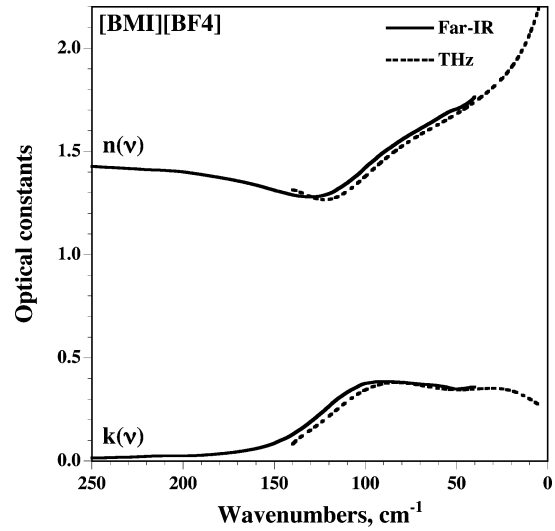

Figure 3. Comparison of the optical constants of [BMI][BF_4] determined in the present work (solid lines) and by Yamamoto et al.[9] (dotted lines).

Optical constants of [BMI][BF_4] have already been determined in the THz region.[9] We have tried to see whether a satisfactory agreement is obtained between these THz data and our optical constants measured in the far-IR region. The comparison of the two studies reported in Figure 3 shows that the goal of obtaining quantitatively consistent data has been reached. In particular, similar shapes and intensities are found for the mode located at ~100 cm^{-1}. The overall red shift of 7 cm^{-1} observed between the IR and THz data has to be attributed to a calibration problem with this latter technique because absolute wavenumbers are measured, on principle, by Fourier transform IR spectroscopy. Because numerous dielectric measurements are also available in the continuation of the THz region, the optical constants of some ILs are now known from the mid-IR to the GHz. This quantitative approach is a prerequisite before envisaging a unified description of the IL dynamics in the required extended time domain. As already pointed out, various spectroscopic studies have already been performed, but it is not easy to extract a comprehensive picture of the IL dynamics because each technique has its own specificity and time domain.

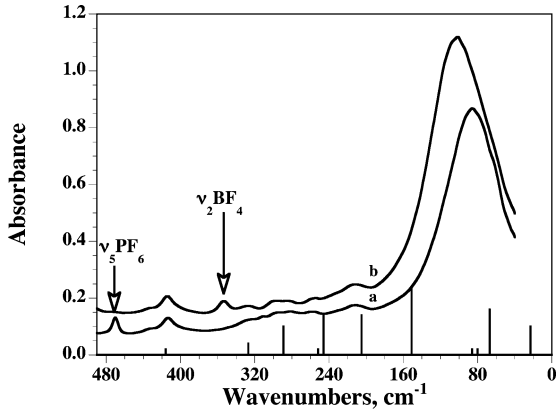

Figure 4. Far-IR spectra of (a) [BMI][PF_6] and (b) [BMI][BF_4] compared with the calculated spectrum of the BMI^+ cation (solid vertical lines).

Discussion

The optical constants reflect any kind of IR absorption due to internal vibrations of the cation and anion and to translational (rattling) and rotational (librations) motions of these ions. It is necessary to identify these different contributions in the 4000−40 cm^{-1} domain and then to analyze the comparatively less well-known external motions.

Internal Vibrations of the Cations and Anions. Numerous vibrational assignments of the considered cations and anions can be found in the literature.[36−45] The different conformers of the $TFSI^-$ anion[36−39] or of the EMI^+ or BMI^+ cations[40−42] have even been spectroscopically identified. The far-IR region has comparatively been less studied and essentially by Ludwig's group.[11−15] As already pointed out, a far-IR broad absorption centered at 80 ± 10 cm^{-1} is observed for the investigated ILs. Note that with lighter anions, such as $N(CN)_2^-$ or SCN^-, Ludwig et al. observed a shift of the band maximum up to 113.5 or 117.6 cm^{-1}, respectively.[15] Whatever the exact interpretation of this absorption, there is a general agreement on the fact that it involves interionic motions. A first question is to know whether low-frequency internal modes of the cation and anion contribute to the whole far-IR absorption. In the [BMI][BF_4] and [BMI][PF_6] spectra, the well-known anion vibrations are all situated above 300 cm^{-1} and easy to identify.[43−45] The presence of the ν_5 vibration of PF_6^- at 470 cm^{-1} and of the ν_2 vibration of BF_4^- at 353 cm^{-1} (Figure 4a,b) is unexpected because these vibrations are IR-inactive for strictly octahedral and tetrahedral anions, respectively. The observed wavenumbers are similar to those of "free" anions in dilute solutions,[43−45] but the weak IR activities indicate that the BF_4^- and PF_6^- anions are submitted to an anisotropic electrostatic field within the ILs. Long range Coulombic interactions are certainly the dominant interionic interactions in ILs, but weak charge transfer interactions may also exist.[46] They would result in a change of the anion electron charge distribution compared with the "free" anion and produce weak activity of initially forbidden vibrations without causing noticeable frequency shifts and degeneracy liftings. We have previously shown that the ν_1 vibration of PF_6^- at 741 cm^{-1}, also activated in [BMI][PF_6], disappears by dilution in polar solvents as a result of the formation of solvent-separated ion pairs (SSIPs) and of the recovery of the octahedral symmetry.[2] On the contrary, the ν_1 band is maintained and even slightly increased in solvents of low dielectric constant as if ion pairs (IPs) had been solvated.

Once the anion internal vibrations are identified, all of the other weak bands in Figure 4a,b can to be assigned to internal vibrations of the BMI^+ cation. A comparison with the DFT calculated spectrum of the more abundant gauche-anti (GA) conformer confirms the presence of weak BMI^+ absorption bands observed at 414, 327, 282, 257, and 212 cm^{-1}. These vibrations involve a complex mixing of torsion and deformation modes. Furthermore, some of these motions, such as the torsion of the substituted methyl groups, are expected to occur in an anharmonic potential with a very low barrier.[17] The harmonic approximation is clearly insufficient to take these weakly hindered rotations into account. However, we are mainly interested here by the fact that these vibrations are scarce below 100 cm^{-1} with a weak intensity compared with the broad absorption due to interionic motions. The exact nature of the latter is not known because it depends on the very local structure of the IL and on the long-range interactions between these local structures. By analogy to what happens in isotropic glasses and also for simplicity the broad far-IR absorption is hereafter called density of states (DOS).

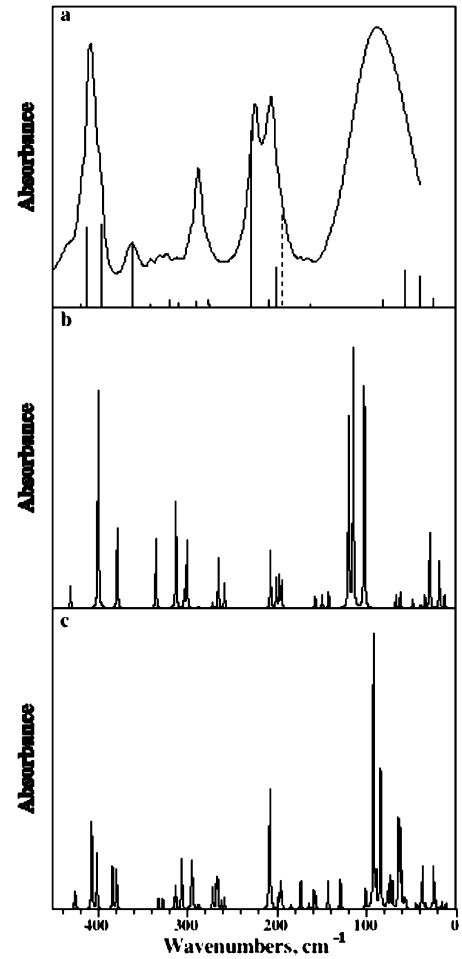

Figure 5. (a) Experimental and calculated IR spectra of [MMI][TFSI]. The calculated IR spectra of the $TFSI^-$ anion of C_2 conformation (solid vertical lines) and of the MMI^+ cation (dotted vertical lines) are given below the experimental spectrum. (b) Calculated IR spectrum for a single ion pair of [MMI][TFSI]. (c) Calculated IR spectrum for an ion pair dimer of [MMI][TFSI].

In the [MMI][TFSI] spectrum (Figure 5a), only seven intramolecular vibrations of the cation are expected below 450 cm^{-1}, and only one of these transitions, calculated at 193 cm^{-1}, has significant intensity. All other lines are due to the $TFSI^-$ anion, and they are well reproduced by the calculated spectrum of the more abundant transoid conformer of C_2 symmetry. Some of us have previously shown that the same spectral range in

Raman is very well adapted for a spectroscopic distinction between the two conformers.[37,38] Only four anion internal modes are calculated below 100 cm^{-1}, and they have weak intensities compared with the DOS profile. This is well illustrated by the calculated spectra of IP and $(IP)_2$ species (Figure 5b,c).

Intermolecular Vibrations. In addition to the weakly perturbed internal modes of the cations and anions, new intense transitions due to the intermolecular vibrations appear below 100 cm^{-1}. Ludwig et al. have previously presented frequency calculations for $[EMI][N(CN)_2]_n$ clusters with $n = 2, 4, 6, 8$ that reproduce satisfactorily the experimental far-IR spectrum.[11,15] They do not comment why a simple ion pair is disregarded, but the results of Figure 5 show that the observed DOS is indeed better reproduced by the $(IP)_2$ spectrum (Figure 5c) than by the IP one (Figure 5b). The more intense lines are situated at 115 cm^{-1} for the IP and at 92 cm^{-1} for the $(IP)_2$ species compared with 88 cm^{-1} for the experimental spectrum. The calculated spectra for $n = 4, 6, 8$ would exhibit more and more transitions in this region, but according to Ludwig et al., the envelope of these transitions remains at about the same position as that for $n = 2$.[11,14,15] In other words, there are more differences between the IP ($n = 1$) and $(IP)_2$ ($n = 2$) spectra than between the spectra of the $n = 2$ and $n > 2$ clusters. The position of the IP transition at higher wavenumbers follows from the more localized and directive interactions in this system compared with the $(IP)_n$ species, where cooperative effects produce a gathering of all transitions around a mean position at lower wavenumbers. Nevertheless, no definitive conclusion on the structuration in ILs can be drawn from the results of Figure 5. Further theoretical modeling is clearly needed to reproduce the experimental profiles.

The more important aim of the present work was to measure quantitatively far-IR profiles and to compare the response of different ILs. For this comparison, it is necessary to bring the intensities, expressed in either $k(\nu)$ or absorbance, to a common concentration scale. Indeed, the molar concentration of the investigated ILs varies, as shown in Table 1. The normalization applied to the TFSI derivatives shows that apart from a band of the $BMMI^+$ cation that shows up at 276 cm^{-1}, the absorption bands at 408, 362, 288, 224, and 206 cm^{-1} due to the anion internal modes have very similar intensities in the four ILs (Figure 6).

The similarity of the four DOSs intensities is much more surprising. Indeed, if this DOS was essentially due to a stretching motion of the $C_{(2)}H\cdots TFSI^-$ hydrogen bond, as claimed by Ludwig et al.,[11−15] then the change of the $C_{(2)}H$ group by a $C_{(2)}CH_3$ group should give a much less intense DOS in [BMMI][TFSI] than in [BMI][TFSI]. The molar concentrations of these two ILs are a little different (Table 1), and the normalization does not modify fundamentally an observation already apparent on the direct absorbance spectra. Although using a constant path length, Köddermann et al. report strong differences between the far-IR spectra of [EMI][TFSI] and [EMMI][TFSI], where $EMMI^+$ is the 1-ethyl-2,3-dimethylimidazolium cation.[13] Here again the concentration normalization (3.87 and 3.69 M, respectively) would have a small effect on the relative intensities. It seems quite unlikely that the $TFSI^-$ internal modes at 206 and 224 cm^{-1} can be twice as weak in [EMMI][TFSI] as in [EMI][TFSI] (Figure 2 of ref 13). Furthermore, the reported [EMMI][TFSI] spectra vanish when the temperature is varied between 313 and 353 K. It is certainly very difficult to obtain a homogeneous liquid film by heating compounds such as [EMMI][TFSI], which are solid at room temperature. It is why we have prioritized ILs that are liquid at room temperature (RTILs).

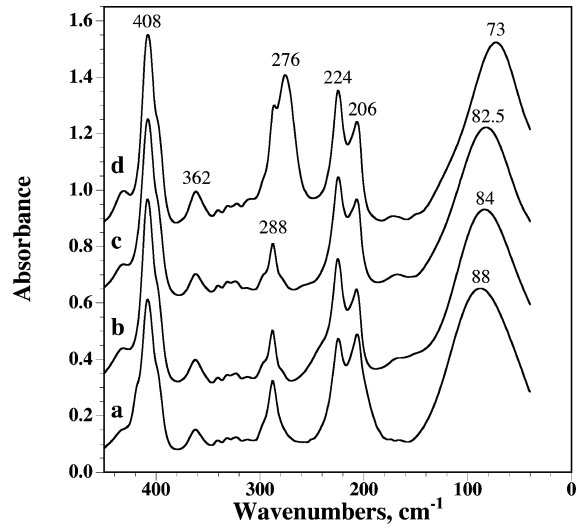

Figure 6. Far-IR spectra of (a) [MMI][TFSI], (b) [EMI][TFSI], (c) [BMI][TFSI], and (d) [BMMI][TFSI] at room temperature under a thickness of 50 μm. Spectrum a is taken as a reference, and the intensities of spectra b−d are multiplied by the factors (4.13/3.87), (4.13/3.43), and (4.13/3.27), respectively, to normalize the concentrations. (See Table 1.) The spectra are shifted upward by 0.3 absorbance units for more clarity.

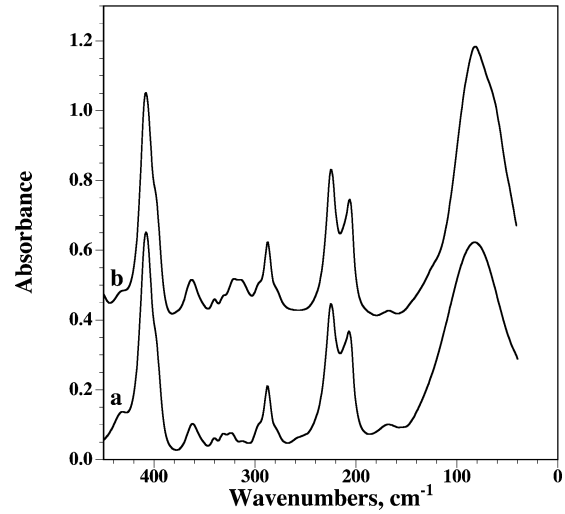

Figure 7. Comparison of the far-IR spectra of (a) [BMI][TFSI] and (b) $[NBuMe_3][TFSI]$ after the bands due to the $TFSI^-$ internal vibrations in the 150−450 cm^{-1} region have been normalized.

As a further experimental contribution to the interpretation of far-IR spectra, a nonimidazolium IL, namely, the $[NBuMe_3][TFSI]$ compound, has also been investigated. Its far-IR spectrum is compared with the [BMI][TFSI] one in Figure 7. The two DOSs have similar intensities and are centered at about the same position, although the $NBuMe_3^+$ cation can hardly establish hydrogen bond interactions with the anion. These DOSs can be viewed as envelopes of the lattice vibrations existing in the solid state, and they are mainly governed by electrostatic interactions.

Conclusions

As far as we know, the optical constants of ILs have been determined for the first time in the 4000−40 cm^{-1} range, and they have been successfully connected to the results obtained

independently in the THz and dielectric domains. Therefore, the dielectric response of ILs becomes available in a wide time domain, from fast internal vibrations to ac and dc. conductivities. The comparison of the far-IR DOSs of various ILs involving the weakly coordinating anions $TFSI^-$, PF_6^-, and BF_4^- shows that the intermolecular vibrations produce a broad absorption centered at 80 ± 10 cm^{-1}, independently of the presence of acidic CH bonds on the imidazolium cation. Theoretical developments are now needed to reproduce the observed profiles. Double ion pairs seem to give a better agreement than simple ion pairs, but it is clear that a gas-phase model for $(IP)_n$ clusters is not a good approximation to take into account a fundamental feature of ILs, namely, the presence of long-range interaction forces. A possible improvement would be the introduction of a continuum polarizable model of solvation.[47] However, even sophisticated DFT calculations do not involve the dynamical aspects, that is, the lifetimes of the nanostructures formed within the ILs and the exchanges between different species. Molecular dynamics simulations may then constitute a more appropriate approach.[48] In any case, we believe that accurate experimental results are an essential prerequisite for any theoretical development. The direct comparison of the far-IR profiles of various ILs shows, for example, that the DOS of the intermolecular motions is essentially governed by electrostatic interactions. As far as weakly coordinating anions are concerned, hydrogen bonding interactions seem to play a minor role, even with imidazolium-based ILs, a conclusion already reached from the study of the CH stretching vibrations of these imidazolium derivatives.[49]

Acknowledgment. We thank the CNRS (Chemistry Department) and the Région Aquitaine for financial support in FTIR and optical equipments. We also acknowledge computational facilities provided by the Pôle Modélisation of the Institut des Sciences Moléculaires and the M3PEC-Mésocentre of the University Bordeaux 1 (http://www.m3pec.u-bordeaux1.fr), financed by the Conseil Régional d'Aquitaine and the French Ministry of Research and Technology.

Supporting Information Available: Optical constants of the six investigated ILs. This material is available free of charge via the Internet at http://pubs.acs.org.

References and Notes

(1) Bertie, J. E. In *Handbook of Vibrational Spectroscopy*; Chalmers, J. M., Griffiths, P. R., Eds; John Wiley & Sons: Chichester, U.K., 2002; Vol 1, pp 88−100.
(2) Buffeteau, T.; Grondin, J.; Lassègues, J. C. *Appl. Spectrosc.* **2010**, *64*, 112.
(3) Stoppa, A.; Hunger, J.; Buchner, R.; Hefter, G.; Thoman, A.; Helm, H. *J. Phys. Chem. B* **2008**, *112*, 4854.
(4) Buchner, R.; Hefter, G. *Phys. Chem. Chem. Phys.* **2009**, *11*, 8984.
(5) Turton, D. A.; Hunger, J.; Stoppa, A.; Hefter, G.; Thoman, A.; Walther, M.; Buchner, R.; Wynne, K. *J. Am. Chem. Soc.* **2009**, *131*, 11140.
(6) Izgorodina, I. E.; Forsyth, M.; MacFarlane, D. R. *Phys. Chem. Chem. Phys.* **2009**, *11*, 2452.
(7) Nakamura, K.; Shikata, T. *ChemPhysChem.* **2010**, *11*, 285.
(8) Daguenet, C.; Dyson, P. J.; Krossing, I.; Oleinikova, A.; Slattery, J.; Wakai, C.; Weingärtner, H. *J. Phys. Chem. B* **2006**, *110*, 12682.
(9) Yamamoto, K.; Tani, M.; Hangyo, M. *J. Phys. Chem. B* **2007**, *111*, 4854.
(10) Dominguez-Vidal, A.; Kaun, N.; Ayora-Cañada, M. J.; Lendl, B. *J. Phys. Chem. B* **2007**, *111*, 4446.
(11) Fumino, K.; Wulf, A.; Ludwig, R. *Angew. Chem., Int. Ed.* **2008**, *47*, 3830.
(12) Fumino, K.; Wulf, A.; Ludwig, R. *Angew. Chem., Int. Ed.* **2008**, *47*, 8731.
(13) Köddermann, T.; Fumino, K.; Ludwig, R.; Canongia Lopes, J. N.; Pádua, A. A. H. *ChemPhysChem.* **2009**, *10*, 1181–1186.
(14) Wulf, A.; Fumino, K.; Ludwig, R. *Angew. Chem., Int. Ed.* **2010**, *49*, 449.
(15) Wulf, A.; Fumino, K.; Ludwig, R.; Taday, P. F. *ChemPhysChem.* **2010**, *11*, 349.
(16) Iwata, K.; Okajima, H.; Saha, S.; Hamaguchi, H.-o. *Acc. Chem. Res.* **2007**, *40*, 1174.
(17) Triolo, A.; Russina, O.; Hardacre, C.; Nieuwenhuyzen, M.; Gonzalez, M. A.; Grimm, H. *J. Phys. Chem. B* **2005**, *109*, 22066.
(18) Giraud, G.; Gordon, C. M.; Dunkin, I. R.; Wynne, K. *J. Chem. Phys.* **2003**, *119*, 464.
(19) Xiao, D.; Rajian, J. R.; Hines, L. G.; LI, S.; Bartsch, R. A.; Quitevis, E. L. *J. Phys. Chem. B* **2008**, *112*, 13316.
(20) Tariq, M.; Forte, P. A. S.; Costa Gomes, M. F.; Canongia Lopes, J. N.; Rebelo, L. P. N. *J. Chem. Thermodyn.* **2009**, *41*, 790.
(21) Bonhôte, P.; Dias, A. P.; Papageorgiou, N.; Kalyanasundarn, K.; Gratzel, M. *Inorg. Chem.* **1996**, *35*, 1168.
(22) Abelès, F. *Ann. Phys.* **1948**, *3*, 504.
(23) Hansen, W. N. *J. Opt. Soc. Am.* **1968**, *58*, 380.
(24) Ohta, K.; Ishida, H. *Appl. Opt.* **1990**, *29*, 2466.
(25) Yamamoto, K.; Ishida, H. *Appl. Spectrosc.* **1994**, *48*, 775.
(26) Bardwell, J. A.; Dignam, M. J. *J. Chem. Phys.* **1985**, *83*, 5468.
(27) Dignam, M. J. *Appl. Spectrosc. Rev.* **1988**, *24*, 99.
(28) Dignam, M. J.; Mamiche-Afara, S. *Spectrochim. Acta, Part A* **1988**, *44*, 1435.
(29) Huang, J. B.; Urban, M. W. *Appl. Spectrosc.* **1992**, *46*, 1666.
(30) Buffeteau, T.; Blaudez, D.; Péré, E.; Desbat, B. *J. Phys. Chem. B* **1999**, *103*, 5020.
(31) Blaudez, D.; Boucher, F.; Buffeteau, T.; Desbat, B.; Grandbois, M.; Salesse, C. *Appl. Spectrosc.* **1999**, *53*, 1299.
(32) Buffeteau, T.; Le Calvez, E.; Castano, S.; Desbat, B.; Blaudez, D.; Dufourcq, J. *J. Phys. Chem. B* **2000**, *104*, 4537.
(33) Frisch, M. J., et al. *Gaussian 03*, revision B.04; Gaussian, Inc.: Pittsburgh, PA, 2003.
(34) Tsuzuki, S.; Tokuda, H.; Mikami, M. *Phys. Chem. Chem. Phys.* **2007**, *9*, 4780.
(35) Danten, Y.; Cabaço, M. I.; Besnard, M. *J. Phys. Chem. A* **2009**, *113*, 2873.
(36) Rey, I.; Johansson, P.; Lindgren, J.; Lassègues, J. C.; Grondin, J.; Servant, L. *J. Phys. Chem. A* **1998**, *102*, 3249.
(37) Herstedt, M.; Smirnov, M.; Johansson, P.; Chami, M.; Grondin, J.; Servant, L.; Lassègues, J. C. *J. Raman Spectrosc.* **2005**, *36*, 762.
(38) Herstedt, M.; Henderson, W. A.; Smirnov, M.; Ducasse, L.; Servant, L.; Talaga, D.; Lassègues, J. C. *J. Mol. Struct.* **2006**, *783*, 145.
(39) Fujii, K.; Fujimori, T.; Takamuku, T.; Kanzaki, R.; Umebayashi, Y.; Ishiguro, S.-i. *J. Phys. Chem. B* **2006**, *110*, 8179.
(40) Umebayashi, Y.; Fujimori, T.; Sukizaki, T.; Asada, M.; Fujii, K.; Kanzaki, R.; Ishiguro, S.-i. *J. Phys. Chem. A* **2005**, *109*, 8976.
(41) Lassègues, J. C.; Grondin, J.; Holomb, R.; Johansson, P. *J. Raman Spectrosc.* **2007**, *38*, 551.
(42) Holomb, R.; Martinelli, A.; Albinsson, I.; Lassègues, J. C.; Johansson, P.; Jacobsson, P. *J. Raman Spectrosc.* **2008**, *39*, 793.
(43) Nakamoto, K. *Infrared and Raman Spectra of Inorganic and Coordination Compounds*, 5th ed.; Wiley: New York, 1997.
(44) Chabanel, M.; Legoff, D.; Touaj, K. *J. Chem. Soc. Faraday Trans.* **1996**, *92*, 4199.
(45) Burba, C. M.; Frech, R. *J. Phys. Chem. B* **2005**, *109*, 5161.
(46) Katoh, R.; Hara, M.; Tsuzuki, S. *J. Phys. Chem. B* **2008**, *112*, 15426.
(47) Palomar, J.; Ferro, V. R.; Gilarranz, M. A.; Rodriguez, J. J. *J. Phys. Chem. B* **2007**, *111*, 168.
(48) Del Popolo, M. G.; Lynden-Bell, R. M.; Kohanoff, J. *J. Phys. Chem. B* **2005**, *109*, 5895.
(49) Lassègues, J. C.; Grondin, J.; Cavagnat, D.; Johansson, P. *J. Phys. Chem. A* **2009**, *113*, 6419.

JP102087M